CrossMark

Research Article

Nanoencapsulation Improves Scavenging Capacity and Decreases Cytotoxicity of Silibinin and Pomegranate Oil Association

Marila C. L. Marchiori,[1] Cristina Rigon,[1] Priscila M. Copetti,[2] Michele R. Sagrillo,[2] and Letícia Cruz[1,3]

Abstract. Silibinin (SB) and pomegranate oil (PO) present therapeutic potential due to antioxidant activity, but the biological performance of both bioactives is limited by their low aqueous solubility. To overcome this issue, the aim of the present investigation was to develop nanocapsule suspensions with PO as oil core for SB encapsulation, as well as assess their toxicity *in vitro* and radical scavenging activity. The nanocapsule suspensions were prepared by interfacial deposition of preformed polymer method. SB-loaded PO-based nanocapsules (SBNC) showed an average diameter of 157 ± 3 nm, homogenous size distribution, zeta potential of −14.1 ± 1.7 mV, pH of 5.6 ± 0.4 and SB content close to 100%. Similar results were obtained for the unloaded formulation (PONC). The nanocapsules controlled SB release at least 10 times as compared with free SB in methanolic solution. The SBNC scavenging capacity *in vitro* was statistically higher than free SB ($p < 0.05$). Cell viability in monocytes and lymphocytes was kept around 100% in the treatments with SBNC and PONC, while the SB and the PO caused a decrease around 30% at 50 µM (SB) and 724 µg/mL (PO). Protein carbonyls and DNA damage were minimized by SB and PO nanoencapsulation. Lipid peroxidation occurred in nanocapsule treatments regardless of the SB presence, which may be attributed to PO acting as substrate in reaction. The free compounds also caused lipid peroxidation. The results show that SBNC and PONC presented adequate physicochemical characteristics and low toxicity against human blood cells. Thereby, this novel nanocarrier may be a promising formulation for therapeutic applications.

KEY WORDS: silymarin; vegetable oil; nanoparticles; antioxidant; cytotoxicity.

INTRODUCTION

Silibinin (SB) is a flavonoid isolated from seeds and fruits of milk thistle plant (*Silybum marianum*). Its extract, named silymarin, is a mixture of flavolignan (silibinin, isosilibinin, silydianin, and silychristin) among other components less pharmacologically important. SB is the most abundant and active component which has shown stronger efficacy in treating hepatic injury and most recently has been considered a potential anticancer and chemopreventive agent. Its biological effects have been attributed to anti-inflammatory, antioxidant and immuno-modulatory mechanisms (1,2). Despite SB potential, it has low aqueous solubility which impairs its oral bioavailability (3,4). Besides, because it is a polyphenolic compound with apolar characteristics, it has at the same time difficulty to solubilize in oils and water (5). Such physicochemical characteristics make SB a candidate for nanoencapsulation to circumvent these limitations. With this respect, some recent studies showed SB-loaded matrix nanoparticles with controlled release, improved solubility, bioavailability and biological effects (6–8).

The pomegranate oil (PO) is rich in unsaturated fatty acids, including punic, oleic, linoleic and palmitic acids, that have an important role in preventing cardiovascular diseases (9). Due to the phenolic compounds and unsaturated fatty acids, it has the capacity to scavenge free radicals and reduce reactive species of oxygen (10). With respect to cancer, PO has preventive and antiproliferative activities (11,12). Nanoemulsion and lipid nanoparticles have been developed to improve neuroprotective effect, antioxidant capacity, photoprotection and antiglioma activity (13–15). The association between oil and active molecule-loaded nanostructured systems has improved the effectiveness of both by a synergistic effect (16,17).

As already mentioned, nanotechnology can improve the performance of drugs and vegetable oils. Among the nanoparticulate systems, the nanocapsules have recognized capacity for improving drug biological effects. The nanocapsules present core–shell architecture, able to act as

[1] Laboratório de Tecnologia Farmacêutica, Programa de Pós-graduação em Ciências Farmacêuticas, Centro de Ciências da Saúde, Departamento de Farmácia Industrial, Universidade Federal de Santa Maria, Santa Maria, 97105-900, Brazil.
[2] Centro Universitário Franciscano, Santa Maria, Brazil.
[3] To whom correspondence should be addressed. (e-mail: leticiacruz@smail.ufsm.br)

aaps

a drug reservoir. The shell is composed by a polymer which acts as a membrane controlling the drug release. The core, usually oily, differentiates nanocapsules from nanospheres (18). Vegetable oils have been chosen as raw materials to form a nanocapsule core due to their important biological activities. In this way, PO in nanocapsules serves as a structural and functional component which could contribute to a better therapeutic outcome (19–21).

The improvement in the pharmacological effect and in the physical and chemical properties is only advantageous, if it does not result in an increased toxicity. Although many plant elements are recognized as non-toxic and safe at therapeutic doses, the nanocapsule toxicity should be checked. The growing interest in nanotechnology as a tool to improve drug clinical efficacy is linked to the need of understanding the nanosystem toxicity. The toxicology field is frequently searching for protocols to evaluate cytotoxicity and genotoxicity, which can also be related to the primary components of the nanoparticles and not only to the active component. Mononuclear blood cells (monocytes and lymphocytes) are involved in the inflammatory process, and are the first to react when the body suffers an injury, being considered toxicity biomarkers. So, to know how the formulations influence these cells is extremely relevant (18,22).

In a recent study, our group demonstrated that SB-loaded PO-based nanocapsules exhibited anti-inflammatory effects on skin damage UVB radiation induced in mice (23). Considering the nanotechnology issues, this study aimed to detail the SB-loaded PO-based nanocapsule preparation and characterization, as well as to evaluate their cytotoxicity in human blood cells.

MATERIALS AND METHODS

Materials

SB, 3-(4,5-dimethythiazol-2-yl)-2,5-diphenyltetrazolium bromide (MTT), 1-1-diphenyl-2-picrylhydrazyl (DPPH), 2,4-dinitrophenylhydrazine (DNPH), and Histopaque-1077® were purchased from Sigma-Aldrich Co. (St. Louis, USA). The PO was obtained from Florien (Brazil). Polysorbate 80 and sorbitan monooleate were acquired from Brasquim (Porto Alegre, Brazil). Ethyl celullose was donated from Colorcon (Cotia, Brazil). Fetal bovine serum (FBS) was obtained from Gibco (Carlsbad, USA). Thiobarbituric acid (TBA) was purchased from Merck (Darmstadt, Germany). The culture medium RPMI was purchased from Vitrocell (Campinas, Brazil). All other chemicals and solvents presented pharmaceutical grade.

Methods

Analytical Method

The analytical method was developed on LC-10A HPLC system (Shimadzu, Japan) equipped with LC-20AT pump, UV-Vis SPD-M20A detector, CBM-20A system controller, and SIL-20A HT valve sample automatic injector. The separation was achieved using a Kinetex C_{18} Phenomenex column (250 mm × 4.60 mm, 5 μm; 110 Å) coupled to a C_{18} guard column at room temperature. The SB detection was performed at 288 nm and the isocratic mobile phase (acetonitrile/water pH 3.5) (40:60, *v/v*) at 1 mL/min flow rate. The method was linear (*r* = 0.9999), specific, accurate (98.25 to 101.87%), precise, and robust (relative standard deviation was <2%).

Dissolution/Swelling of Polymer Films and SB Solubility

Polymer films were prepared by ethyl cellulose (EC) dispersion in acetone, followed by its evaporation at room temperature. Fragments about 35 mg of the polymer film were immersed in PO at room temperature, during 60 days, in order to evaluate the oil's ability to solubilize or swell the EC film (24). In predetermined intervals, the films were removed from the contact with the oil and dried with an absorbing paper. Weight variation was determined using an analytical balance. The experiment was conducted in triplicate.

To evaluate the SB solubility in PO, an excessive SB amount was added to 3 mL of oil, kept under magnetic stirring for 12 h and centrifuged at 3000 rpm for 10 min. A supernatant aliquot was diluted with methanol and quantified by the HPLC method described above.

Nanocapsule Preparation and Characterization

SB-loaded polymeric nanocapsules (SBNC) were prepared in triplicate of batch by interfacial deposition of preformed polymer (25). An organic phase containing 0.077 g of sorbitan monooleate, 0.3 g of PO, 0.1 g of EC and 0.01 g of SB were dissolved in 50 mL of acetone. This organic solution was injected into 50 mL of an aqueous phase containing 0.077 g of polysorbate 80 under moderate magnetic stirring during 10 min. Acetone was removed, and the aqueous phase was concentrated by evaporation at 40°C under reduced pressure to obtain 10 mL. The final theoretical SB concentration in the aqueous nanocapsule suspension was 1 mg/mL, and the oil content was 3%. For comparison purposes, blank nanocapsule suspensions (PONC) were prepared in a similar way, but without SB addition.

The total SB content in nanocapsule suspensions was assayed by diluting a sample aliquot in 10 mL methanol and subjecting it to sonication for 5 min. Samples were filtered through a 0.45 μm membrane and injected into the HPLC system using the method described above. For the determination of the encapsulation efficiency, a sample aliquot was placed in a 10,000 MW centrifugal device (Amicon® Ultra, Millipore) and free drug was separated from the nanostructures by ultrafiltration/centrifugation technique at 7000 rpm for 10 min. The difference between the total and the free SB concentrations, determined in the SBNC and in the ultrafiltrate, respectively, was calculated as the encapsulation efficiency (EE%) according to the following equation:

$$EE\% = \frac{\text{Total SB content} - \text{Free SB content}}{\text{Total SB content}} \times 100 \qquad (1)$$

Particle sizes and polydispersity indexes (PDIs) were measured by photon correlation spectroscopy (Zetasizer Nano series, Malvern Instruments, UK). Zeta potentials (ZP) were evaluated by microelectrophoresis, using the same

instrument. pH values were determined immersing the electrode of a potentiometer (Model pH 21, Hanna Instruments, Brazil) in the aqueous suspensions. The analyses of these parameters were performed at room temperature in triplicate.

In order to further support the size recorded, scanning electron microscopy was performed. Nanocapsules were previously lyophilized using lactose (cryoprotectant), and the samples were gold sputtered and subsequently analyzed using an accelerating voltage of 5 kV (scanning microscope Vega3, Tescan).

In Vitro SB Release

The SB release from nanocapsules was studied by the dialysis diffusion technique. One milliliter of SBNC was placed in a dialysis bag (10,000 Da), and this system was immersed in 200 mL phosphate buffer (pH 7.4) at 37°C, under continuous magnetic stirring. At predetermined intervals, 1 mL of the release medium was withdrawn and replaced by the same volume of fresh medium, to maintain the *sink* conditions. The amount of SB released was assessed by HPLC, using the same chromatographic conditions previously described. For comparative purposes, the SB methanolic solution was submitted to the *in vitro* release assay. SB is very soluble and stable in methanolic solution. SB (0.01 g) was dissolved in methanol (10 mL) to form a clear and colorless solution (1 mg/mL). The experiment was conducted in triplicate.

In order to understand the mathematical behavior of the release profile and mechanism of SB release, the data was fitted to first order (Eq. (2)) and Korsmeyer–Peppas (Eq. (3)), respectively. The half-life of first-order kinetics was calculated from Eq. (4).

$$C = C_0.e^{-kt} \tag{2}$$

$$ft = a.t^n \tag{3}$$

$$t_{1/2} = 0.693 \big/ k \tag{4}$$

where C is the concentration at time t, C_0 is the SB initial concentration, k is the kinetic rate constant, $t_{1/2}$ is the time to release 50% of SB, ft is the SB fraction released at time t (hours), a is a constant which incorporates structural and geometric characteristics of the release system, and n is the exponent that indicates the drug release mechanism [26]. The Scientist 2.0 software (MicroMath®, USA) was used to perform the mathematical modeling.

DPPH Radical Scavenging Capacity Estimation

In this study, we evaluated the radical scavenging of SBNC, PONC, SB and PO. The SBNC and SB were diluted at 1, 5, 10 and 50 μM concentrations. PONC and PO were also diluted, but their concentrations were expressed in terms of the amount of oil being 14.5, 72.4, 145 and 724 μg/mL. The colloidal suspensions were diluted in water and SB and PO in ethanol. The radical scavenging capacity was based on the

method described by Serpen and co-workers with minor modifications [13,27]. The samples were incubated with 1.5 mL DPPH reagent at room temperature. After 30 min, the absorbance values were measured at 518 nm and expressed as percentage of scavenging capacity following Eq. (5):

$$\%SC = 100 - \frac{(Abs - Abb) \times 100}{Abc} \tag{5}$$

where

%SC	scavenging capacity in percentage
Abs	sample incubated with DPPH absorbance
Abb	sample absorbance (without DPPH)
Abc	control absorbance (DPPH absorbance)

Viability, Genotoxicity, and Oxidative Effects on Mononuclear Blood Cells

Blood Collection. The human blood was used to perform the experiments. The protocol was approved by the committee for research with humans (CAAE:31211214.4.0000.53306) with no identifying data. Peripheral blood samples were obtained from healthy volunteers by vein puncture using a top Vacutainer (BD Diagnostics, Plymouth, UK) and heparin tubes. The Histopaque-1077® density gradient was used to separate mononuclear cells using 4 mL blood samples. After separation, the cells were transferred to culture media containing 5 mL RPMI with 10% fetal bovine serum and 1% penicillin and streptomycin. The cells were cultured at an initial density of 2×10^5 cells/mL and then incubated with SBNC, PONC, SB and PO for 72 h at 37°C in a 5% humidified CO_2 atmosphere. The working concentrations were 1, 5, 10 and 50 μM for the SBNC and SB. PONC were diluted as the SBNC; however, the concentrations were expressed in terms of PO, being 14.5, 72.4, 145 and 724 μg/mL. The samples were diluted in RPMI. Hydrogen peroxide was used as positive control of damage. Negative control was performed by incubating cells with RPMI.

Cell Viability. Cell viability was evaluated using a colorimetric assay that measures the reduction of 3-(4,5-dimethythiazol-2-yl)-2,5-diphenyltetrazolium bromide (MTT) by mitochondrial succinate dehydrogenase. Cell viability was expressed as a percentage of the negative control value. The MTT was dissolved in phosphate buffer (pH 7.4) (5 mg/mL), added into a microplate containing the sample treatments, and incubated for 3 h at 37°C protected of light. The absorbance at 540 nm was read. This assay was performed in triplicate for each treatment.

Comet Assay. The genotoxicity evaluation was performed by Comet assay. This analysis was adapted following the protocol described by Garcia and co-workers [28]. After the incubation, on a glass plate covered with a layer of 1.5% agarose, samples were deposited already suspended in agarose of low melting point. The material was immersed in

lysis solution for the removal of membrane and cytoplasm. The slides were incubated in alkaline electrophoresis buffer and subjected to electrophoresis for 30 min at 25 V and 300 mA. To analyze the genetic material, neutralization, fixation, and coloring processes were carried out. Each slide was evaluated by optic microscopy, and the cells were classified according to the nuclei format into four damage classes, varying from 0 (no damage) to 4 (maximum damage).

Lipid Peroxidation. The evaluation of lipid peroxidation induced by samples was performed by thiobarbituric acid (TBA) reaction with malondialdehyde (MDA), the main product of lipid peroxidation. After incubation, 1 mL suspension cell was centrifuged for 10 min at 1000 rpm. The supernatant was discarded and the pellet was washed with 0.9% NaCl for three times, and 300 µL phosphate buffer (pH 7.4), 100 µL 10 nM BHT and 500 µL 20% trichloroacetic acid were added. This mixture was centrifuged for 5 min at 2000 rpm. Nine hundred microliters of supernatant was mixed with 140 µL water, 300 µL TBA, 60 µL 10% phosphoric acid and incubated for 90 min at 95°C. The reading was performed at room temperature in a spectrophotometer at 532 nm. The results were expressed as nanomoles of MDA/10^6 cells, as in Ferreira and co-workers (13).

Protein carbonyl Assay. The protein damage was determined by the protocol described by Ferreira and co-workers (13). After the incubation, 50 µL of suspension cells was diluted with Tris/HCl buffer (pH 7.4) (1:8) and 20 µL 10 mM DNPH reagent in 2 M HCl was added to an aliquot (1000 µL) of this dilution. For the blank, 20 µL 2 M HCl was used. After, the samples were incubated for 1 h in the dark with vortex mixing every 15 min. Five hundred microliters of denaturing buffer (pH 6.4 + 3% sodium dodecyl sulfate), 2000 µL ethanol and hexane were added to the samples and vortex mixed for 40 s, and then centrifuged for 15 min at 3000 rpm. The pellet was washed with 1 mL ethanol/ethyl acetate (1:1). One thousand microliters of denaturing buffer was added and the tubes were kept in water bath at 40°C until total pellet dissolution. The absorbance was measured at 370 nm and the results were expressed as nanomoles of carbonyl content/10^6 cells.

Statistical Analysis

Formulations were prepared and analyzed in triplicate and the results were expressed as mean ± standard deviation. GraphPad Prism Program, version 6, was the software used for the *t* test and analyses of variance (ANOVA) and post hoc Tukey test. A *p* value <0.05 was considered to be statistically significant.

RESULTS

Dissolution/Swelling of Polymer Films

The initial mass of the polymer films was 36.4 ± 3.1 mg, and that after 60 days of PO contact was 37.3 ± 1.2 mg. However, the statistical analysis pointed out that the observed differences were not significant ($p > 0.05$), indicating that the PO is suitable to form EC nanocapsules.

Physicochemical Characterization

Both colloidal nanocapsule suspensions were milky in appearance and showed the characteristic opalescent bluish reflection resulting from the Brownian motion of the colloidal structures. The mean diameters were lower than 170 nm. Besides, the SB presence did not cause significant difference in particle sizes ($p > 0.05$). The polydispersity indexes were lower than 0.10, which indicates a narrow size distribution. The pH value was slightly acidic. The zeta potential was negative, which is related to the anionic EC feature. SB encapsulation efficiency of SBNC was greater than 96%, which is attributed to the higher SB affinity with the oil core than with the aqueous phase. Table I presents the physicochemical characteristics. A representative image of the developed formulations is shown in Fig. 1. It was possible to visualize the presence of spherical nanostructures at the cryoprotectant surface in the micrograph image.

In Vitro SB Release Study

Figure 2 shows the release profiles of free and nanoencapsulated SB. After 9 h, the release percentages were 31.25 ± 1.52 and 90.15 ± 5.70% for SBNC and SB, respectively. The mathematical modeling indicated that the SB release profile showed higher correlation coefficients for first order and the Korsmeyer–Peppas equation (Table II).

DPPH Radical Scavenging Capacity Estimation

The ability of SBNC, PONC, SB and PO for scavenging DPPH, a stable free radical, was evaluated. Figure 3 presents the DPPH assay results. Radical scavenging activity of SBNC was 80 to 92%. The free SB DPPH scavenging activity was 72 to 80%. There were significant differences between SB and SBNC at all concentrations ($p < 0.05$). The PONC presented radical scavenging activity between 84 and 90%. The PO showed a scavenging capacity between 65 and 85%. Significant differences were observed for the PO and PONC ($p < 0.05$). There was no significant difference between SBNC and PONC ($p > 0.05$).

Cytotoxicity, Oxidative Effects, and Genotoxicity on Mononuclear Cells

Cell viability, based on mitochondrial respiration, was evaluated by MTT reduction assay after 72 h incubation. The blank (PONC) and loaded nanocapsules (SBNC) behaved in the same way, and they were equivalent to the negative control ($p > 0.05$). In contrast, the free compounds caused toxicity in certain concentrations. The cell viability was 78.33 ± 8.40, 71.75 ± 2.47, and 70.42 ± 1.73%, for PO at 145 and 724 µg/mL and SB at 50 µM, respectively, showing statistical difference with the nanostructured formulations at the same concentration and negative control ($p < 0.05$) (Fig. 4).

Most samples had protein carbonyl levels below the negative control. The SB and PO at the highest concentration (50 µM and 724 µg/mL) showed values higher than the

Table I. Characteristics of SB-Loaded (SBNC) and Unloaded (PONC) Nanocapsules

	Mean diameter (nm)	Polydispersity index	Zeta potential (mV)	pH	SB Content (mg/mL)
SBNC	157 ± 3	0.09 ± 0.02	−14.1 ± 1.7	5.63 ± 0.4	1.02 ± 0.03
PONC	160 ± 7	0.09 ± 0.03	−15.8 ± 1.9	6.1 ± 0.2	–

SBNC silibinin-loaded PO-based nanocapsules, *PONC* unloaded nanocapsules

baseline. In particular, the SB caused a prominent damage, which was not observed when this concentration was nanoencapsulated (Fig. 5).

Regarding lipid peroxidation results (Fig. 6), the lowest sample concentrations showed MDA values lower than or equal to the negative control. SB was more toxic than SBNC

Fig. 1. Scanning electron microscopy of lactose (**a**) and nanocapsules (**b**)

at 50 µM. The behaviors of PONC and SBNC were similar, at the largest concentration. The free oil showed more extensive peroxidation levels, which could be observed at 145 and 724 µg/mL.

Table III shows the results of the comet assay. The evaluation of DNA damage is a qualitative data obtained by microscopic evaluation. One hundred nuclei were analyzed over the entire blade for calculating a damage index. For the negative control four nuclei were found with minimal damage (index 0.04). The SBNC showed similar behavior to the negative control. SB at the highest concentration had 17 nuclei with alteration, 3 of which were considered more severe. The PONC damage demonstrated an index of at most 0.08 at 724 µg/mL. The PO had a damage index from 0.02 to 0.29, increasing as their concentration increased.

DISCUSSION

As stated in other studies, an essential condition to the formation of a core–shell structure is the absence of polymer dissolution or swelling by the oil. In order to evaluate if there is an interaction between EC and PO, it is necessary to put them in contact for a period of time. This assessment should be the starting point in the preformulation process because if there is an interaction between the components, the core–shell structure is not formed, and we must replace them (24). The results of dissolution/swelling showed that PO and EC are suitable for being employed together in the nanocapsule preparation. The initial weight of the polymer film remains during the entire monitoring period. There is therefore no risk of dissolution or polymer swelling after obtaining the nanocapsule suspensions. Based on our experience, EC has proven to be an excellent carrier for the preparation of nanocapsules containing vegetable and synthetic oils (19,29). The nanocapsules were prepared by an easy and low-cost method, achieving the characteristics required for a nanoparticulate drug delivery system: high encapsulation efficiency, size around 160 nm, low polydispersity and adequate reproducibility. The same was achieved for PONC. The obtained values are in agreement with those normally found in the literature for systems prepared by interfacial deposition of the preformed polymer method and consistent with drug delivery systems (30). The high encapsulation efficiency of SBNC is attributed to the better affinity of SB with the oil core than the aqueous phase. In accordance with the literature, the SB solubility in water is negligible, while in PO it is 95.26 ± 4.28 µg/mL. The entrapment efficiency of quercetin in EC nanospheres (matrix systems) was around 50%, showing the importance of the oil core in flavonoid encapsulation (31). The SBNC pH was lower than the first acid dissociation constants of SB ($pKa_1 = 6.86$, $pKa_2 = 8.77$, $pKa_3 = 9.62$, and $pKa_4 = 11.38$), predominating the non-
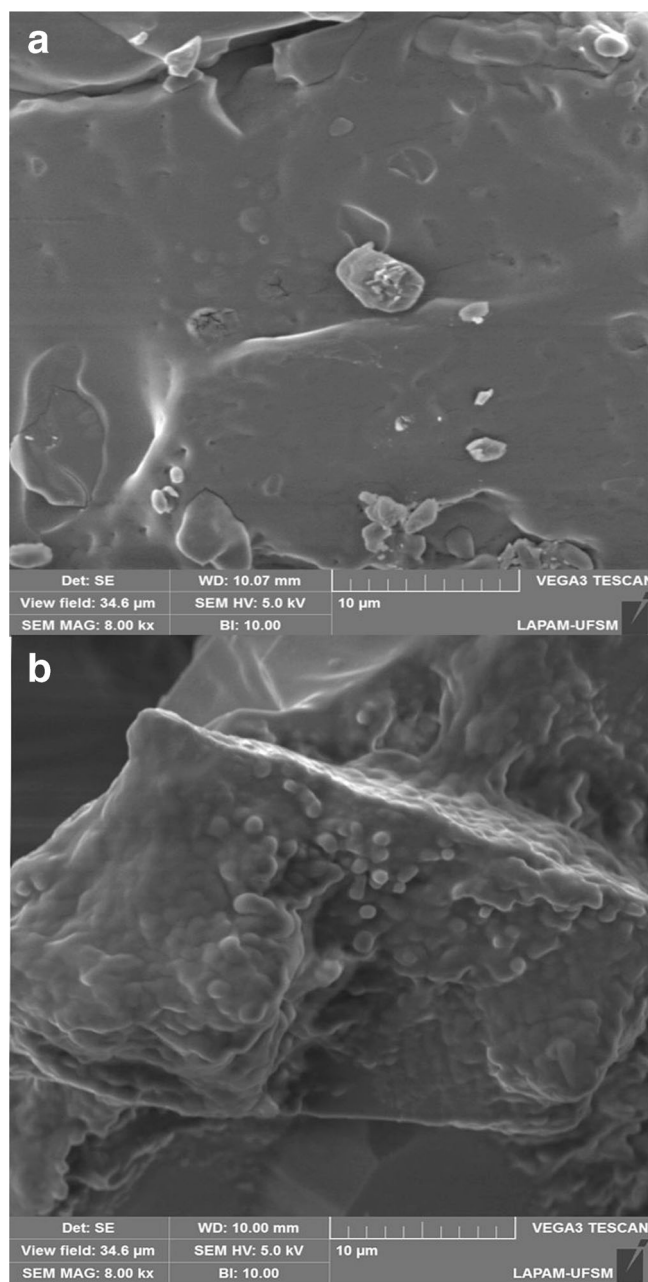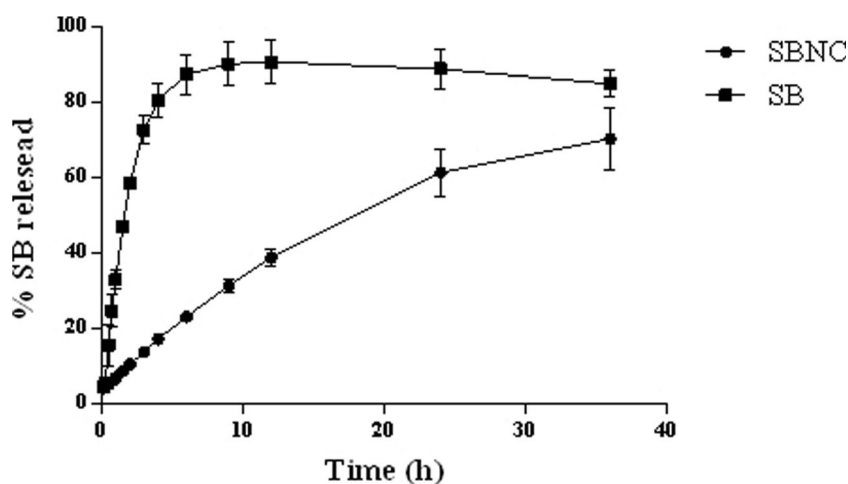
Fig. 2. SB release profiles from methanolic (SB) solution and nanocapsules (SBNC)

ionized molecular form which hinders their partition in the aqueous phase of nanocapsule suspension (32).

The *in vitro* SB release from nanocapsules was performed to elucidate the kinetics and mechanism of SB release, comparatively evaluating the behavior of the methanolic solution. The dialysis membrane used in this study has a porosity cutoff of 10,000 Da, a barrier to the nanocapsules and not to the free drug. Thus, it is inferred that the drug that reaches the receptor medium migrated from the nanocapsule, overtook the dialysis membrane and reached the medium, where it was quantified. The release kinetics of SB-loaded nanocapsules and free form follows the first-order kinetics, which means that there is a linear relationship between the logarithm of drug concentration and time. Because it is a monoexponential function, this equation describes the drug release in a single step, which means that there is no burst effect on SB release profiles and the drug is released in a controlled manner from nanocapsules. Previous studies of our group also showed first-order release kinetics of beclomethasone and acetazolamide from EC nanocapsules (19,29).

Based on the kinetic rate constants and half-lives, the nanoencapsulation controlled SB release around 10 times compared to the drug solution. Being gradually released, the drug may have a prolonged effect, being protected from any degradation and also avoiding physical incompatibilities, such as precipitation or crystallization, with the components of aqueous biological systems. In this sense, due to the high reactivity attributed to polyphenols, a controlled release is very appropriate (33).

Table II. Parameters Calculated for First Order and Korsmeyer–Peppas Equation

	SBNC	SB
First order		
r	0.998 ± 0.001	0.995 ± 0.003
k (h^{-1})	0.042 ± 0.004	0.408 ± 0.011
$t_{1/2}$ (h)	16.61 ± 1.74	1.70 ± 0.04
Korsmeyer–Peppas		
r	0.987 ± 0.001	–
n	0.56 ± 0.02	–

SBNC silibinin-loaded PO-based nanocapsules, *SB* silibinin

The release mechanism of drugs from spherical systems, such as nanocapsules, can be determined by the Korsmeyer–Peppas equation that allows calculating the release exponent "n." According to its value, the release mechanism can be classified as Fickian diffusion ($n = 0.43$), anomalous transport ($0.43 < n < 0.85$) or type II transport ($n \geq 0.85$) (26). In this work, the value of "n" for SBNC was 0.56, corresponding to anomalous transport, which depends on the SB diffusion through the nanocapsule oil core and the effect of external aqueous phase of the colloidal suspension on the polymer wall, causing relaxation of the polymer chains. It is therefore a combination of diffusion and polymer erosion. This mechanism also explains the beclomethasone and repaglinide release from EC nanocapsules (19,34).

Radical scavenging activity is based on the electron-donating capacity to radical DDPH for substances that have several OH groups attached to aromatic rings, such as flavonoids, for example. The compounds capable of donating H are considered scavengers of free radicals. The hydroxyl group bounded to carbon 20 of SB "E" aromatic ring exhibits the major role in this activity (35).

The SB nanoencapsulation increased its antiradical capacity in comparison to the free flavonoid ($p < 0.05$). It must be considered that the SBNC contains PO in its composition, which contributes to the overall scavenging capacity of the nanostructure. It is worth mentioning that the nanocapsules maintain their submicrometric size during the incubation period (data not shown). Some studies have shown that the entrapment of substances may not improve their antioxidant capacity (13,36). Our results demonstrate that the nanoencapsulation can improve scavenging capacity of PO as compared with PONC. This improvement could be explained by the nanometer scale of size, which increases the contact surface, letting the hydrogen donor groups in close proximity with the DPPH molecules (37). A similar observation was described to lipid nanoparticles containing PO (15). Silymarin, the crude extract from which SB is obtained, had its DPPH scavenging property increased after their incorporation into nanosuspensions (450 nm), with IC50 ranging from 13 to 2 mg/mL (38). SB-loaded nanoemulsion (200 to 320 nm) prepared with sunflower oil, castor oil and olive oil did not improve the scavenging capacity of unloaded nanoemulsion (39) similar to that observed in the present
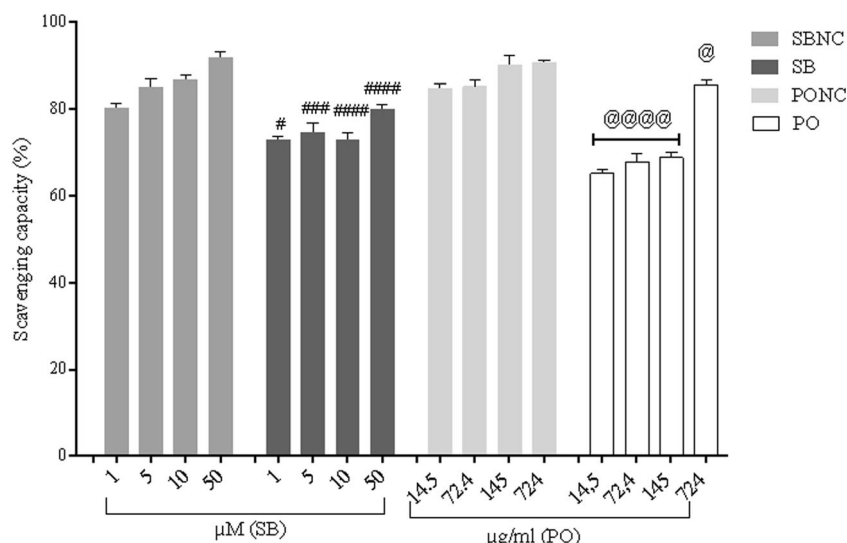
Fig. 3. DPPH radical scavenging capacity. Each *column* represents the mean with standard deviation of triplicates. #Significant difference between SBNC and SB. @Significant difference in PONC and PO

study. Briefly, our results show that SBNC performed better than SB and PO. It is important to emphasize that the oil concentration was 30 times higher than SB concentration (3 and 0.01%, respectively). This qualitative–quantitative composition was necessary to form the nanocapsule oil core with adequate colloidal size. This could explain the same behavior exhibited by both SBNC and PONC ($p > 0.05$).

Mononuclear blood cells (monocytes and lymphocytes) are responsible for the inflammatory and immune response of the body, reacting in the presence of antigens, and, thus, considered toxicity biomarkers (22). The cells were incubated with the SBNC, PONC, SB and PO for lipid peroxidation, protein carbonyl, genotoxicity and cell viability evaluation. MTT assay indicated that SBNC and PONC kept the mitochondrial metabolism of mononuclear cells after the incubation period. In contrast, the free compounds caused depletion in viability, in certain concentrations (PO at 145 and 724 µg/mL and SB in

50 µM), indicating that the nanoencapsulation reverses the toxicity at these doses. In a study performed by Ripoli (2016) (7), the MTT assay revealed, after 72 h of incubation, that SB-loaded liposomes (and unloaded liposomes) were well tolerated by Huh 7.5 cell lines up to 200 µM, while SB (solution) was toxic above 150 µM, showing also that the nanoassociated form is safer. Few studies have evaluated the SB effect on human blood cells. One of these described that the viability was higher than 95% at doses lower than 50 µg/mL, but the technique used was the trypan blue and the exposure time was 24 h (40), differing from the protocol practiced in this study. The SB concentrations used in the present study are in accordance with other protocols testing SB in human blood cell culture (41,42).

Protein carbonyl is a type of damage that cells can undergo in the presence of toxic compounds, like reactive oxygen species (43). The extensive carbonylation observed at 50 µM of SB was reversed when this dose was
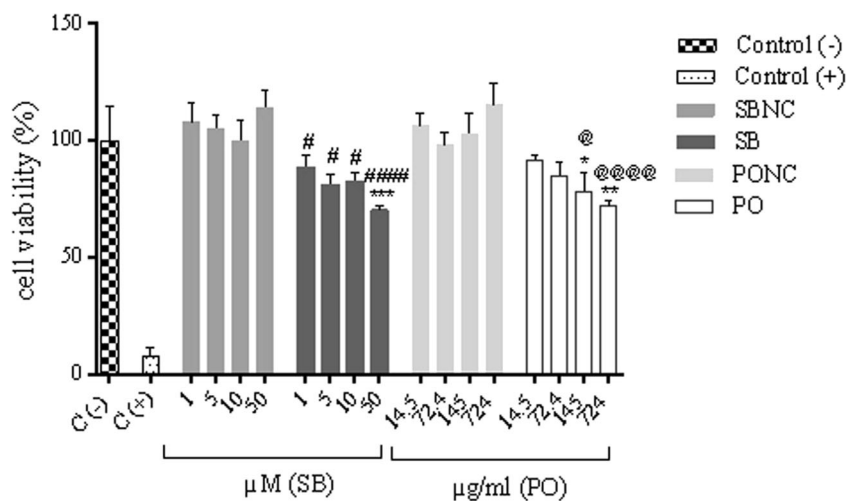

Fig. 4. Cell viability of mononuclear cells after 72 h of incubation by the MTT reduction assay. Each *column* represents the mean with standard deviation of triplicates. *Significant difference between SBNC, SB, PONC, PO and negative control. #Significant difference between SBNC and SB. @Significant difference between PONC and PO
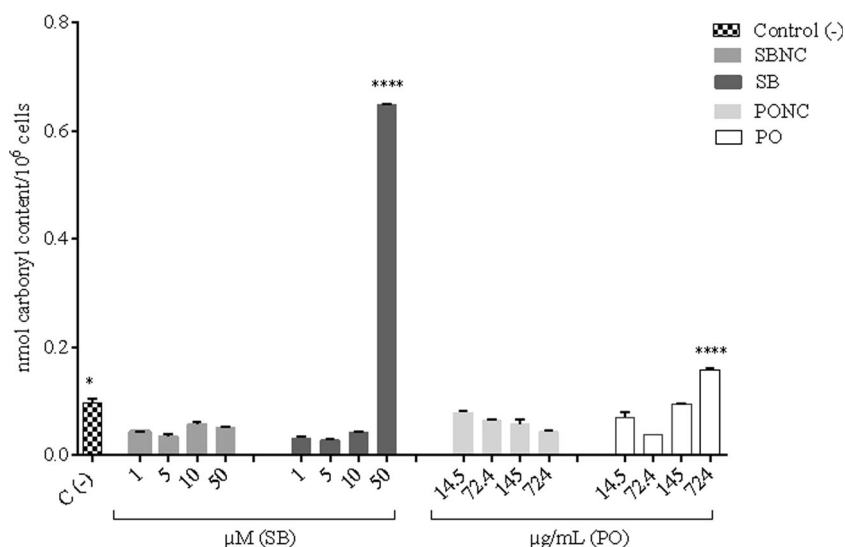
Fig. 5. Carbonyl protein determination in mononuclear cells after 72 h of incubation. Each *column* represents the mean with standard deviation of triplicates. *Represents statistically higher values to the negative control

nanoencapsulated. It is noteworthy that at this concentration the viability declined by $29.6 \pm 1.7\%$ according to MTT results. Thus, it can be inferred that the harm caused by SB involves serious damage to protein cells. The pro-oxidant effect related to SB can justify this increase in protein carbonyls (44). In the biological medium, polyphenols react with transition metals or undergo autoxidation, generating phenoxyl radicals which may initiate lipid peroxidation, DNA damage, and protein oxidation which, in turn, will lead to deleterious effects in biological systems (33). The same happened with PO, which caused higher protein carbonylation than the baseline value, at doses of 145 and 724 μg/mL, which was not observed when the oil was confined in nanoparticles. The comet assay showed DNA damage of mononuclear cells below 10% (damage index = 0.1, value that does not indicate toxicity) (22,28) when treated with SBNC

and PONC at all concentrations tested. On the other hand, SB and PO caused more numerous and severe nuclei damage at the highest dose. When DNA is damaged and adequate repair does not occur, this alteration can be perpetuated. According to the region where the DNA is corrupted, the tumor initiation may occur. Therefore, it is extremely important that the components of a formulation and the active ingredients do not interfere in the genetic integrity, to prevent neoplastic cell generation (2,45). This cytotoxicity results are related to the effective active encapsulation and the controlled SB release, as previously discussed.

The thiobarbituric acid reactive species (TBARS), especially the MDA, are related to oxidative damage in cellular lipid membranes. After the incubation, a certain degree of lipid peroxidation may occur in cells, as seen in the negative control. In pools where cells were treated with the nanocapsules and the
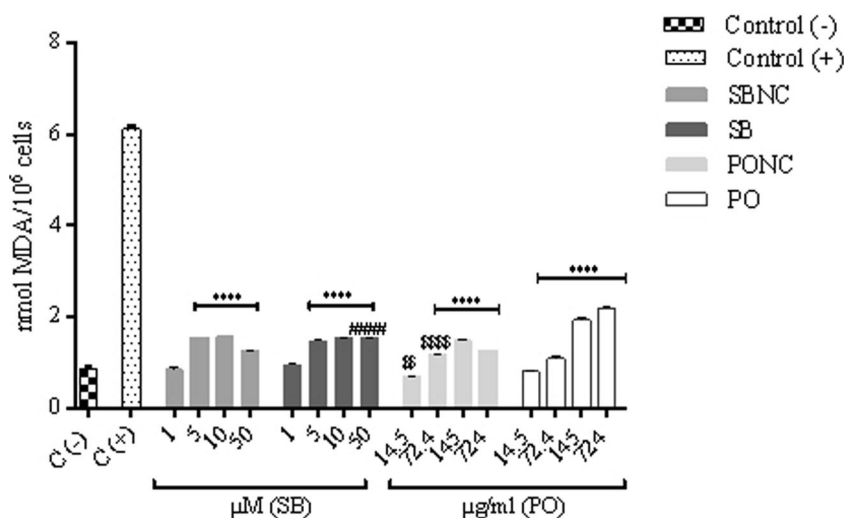

Fig. 6. MDA levels in mononuclear cells after 72 h incubation. Each *column* represents the mean with standard deviation of triplicates. *Represents statistically higher values to the negative control. #Significant difference between SBNC and SB. $Significant difference between SBNC and PONC

Table III. Determination of DNA Cell Damage, Through the Microscopic Analysis, After 72 h Incubation with SBNC, PONC, PO, and SB

	Damage0	Damage1	Damage2	Damage3	Damage4	Damage index
C−	96	4				0.04
C+	50	5	3	30	12	0.5
SBNC 1	96	4				0.04
SBNC 5	97	3				0.03
SBNC 10	95	5				0.05
SBNC 50	96	4				0.04
SB 1	95	5				0.05
SB 5	93	7				0.07
SB 10	92	8				0.08
SB 50	83	14	3			0.17
PONC 14.5	95	5				0.05
PONC 72.4	94	6				0.06
PONC 145	93	7				0.07
PONC 724	92	8				0.08
PO 14.5	98	2				0.02
PO 72.4	96	4				0.04
PO 145	93	7				0.07
PO 724	71	27	2			0.29

Damage index = damaged nuclei/100
SBNC silibinin-loaded PO-based nanocapsules, *PONC* unloaded nanocapsules, *SB* silibinin, *PO* pomegranate oil

PO, the lipid peroxidation reaction may be consuming the oil as a substrate. This possibility is reinforced by the PO results, in which there is a MDA increase in a dose-dependent manner ($p < 0.05$). Along with this, we must also consider the possibility of some oil pro-oxidant effects on the cells, by itself and not as substrate. Still, it is observed that the PO nanoencapsulation significantly decreases ($p < 0.05$) the peroxidation reaction, which is an advantage for the nanocapsules. The nanoencapsulation decreased the injury caused by SB at 50 μM. At lower concentrations, the SBNC promoted an increase in MDA levels, compared with PONC. The literature has been shown that SB causes TBARS increments in renal cells (46) which could explain the peroxidation that occurs due to SB treatments (free or nanoencapsulated). To complement what was discussed, it is worth noting that vegetable oils can suffer lipid peroxidation even being incorporated into nanoemulsions and the SB presence did not interfere in this reaction of the oils (39), as occurred in the present study at 10 and 50 μM.

Cells treated with SB and PO suffered more damage, considering lipid peroxidation, genotoxicity, cell viability and protein carbonyls, showing that these cytotoxicity markers are correlated with each other and contribute to the sample safety understanding. The nanocapsule formulations did not cause protein carbonylation, genotoxicity or decrease in viability. Lipid peroxidation was the only assay that demonstrated values higher than the negative control, but this may be due to the fact that the oil acts as another substrate for the peroxidation reaction. Altogether, the PO and SB incorporation within the nanostructure, which is bounded by the EC polymeric wall, avoids their direct contact with the cells and minimizes their harmful effects.

CONCLUSION

The nanocapsules containing SB and PO were successfully developed. The nanoencapsulation controlled SB release, protected the cells from toxic effects caused by the active ingredients, improved their scavenging capacity *in vitro* and water solubility. Thus, the nanocapsules developed can be considered feasible and safe carriers for SB and PO. Such nanocapsule aqueous suspension is a potential intermediate product for the development of dosage forms.

COMPLIANCE OF ETHICAL STANDARDS

Disclosure of Interests The authors report no conflicts of interest.

REFERENCES

1. Chhabra N, Buzarbaruah S, Singh R, Kaur J. Silibinin: a promising anti-neoplastic agent for the future? A critical reappraisal. Int J Nutr Pharmacol Neurol Dis. 2013;3:206–18.
2. Vaid M, Katiyar SK. Molecular mechanisms of inhibition of photocarcinogenesis by silymarin, a phytochemical from milk thistle (*Silybum marianum* L. Gaertn). Int J Oncol. 2010;36:1053–60.
3. Shakeel F, Anwer MK. Dissolution thermodynamics and solubility of silymarin in PEG 400-water mixtures at different temperatures. Drug Dev Ind Pharm. 2015;41:1819–23.
4. Zhu Y, Wang M, Zhang Y, Zeng J, Omari-Siaw E, Yu J, *et al*. In vitro release and bioavailability of silybin from micelle-templated porous calcium phosphate microparticles. AAPS PharmSciTech. 2015;17:1232–40.

5. Kidd P, Head K. A review of the bioavailability and clinical efficacy of milk thistle phytosome: a silybin-phosphatidylcholine complex (Siliphos®). Altern Med Rev. 2005;10:193–203.

6. Pooja D, Babu Bikkina DJ, Kulhari H, Nikhila N, Chinde S, Raghavendra YM, et al. Fabrication, characterization and bioevaluation of silibinin loaded chitosan nanoparticles. Int J Biol Macromol. 2014;69:267–73.

7. Ripoli M, Angelico R, Sacco P, Ceglie A, Mangia A. Phytoliposome-based silibinin delivery system as a promising strategy to prevent hepatitis C virus infection. J Biomed Nanotechnol. 2016;12:770–80.

8. Wang Y, Zhang L, Wang Q, Zhang D. Recent advances in the nanotechnology-based drug delivery of silybin. J Biomed Nanotechnol. 2014;10:543–58.

9. Mirmiran P, Fazeli MR, Asghari G, Shafiee A, Azizi F. Effect of pomegranate seed oil on hyperlipidaemic subjects: a double-blind placebo-controlled clinical trial. Br J Nutr. 2010;104:402–6.

10. Badea G, Lăcătuşu I, Badea N, Ott C, Meghea A. Use of various vegetable oils in designing photoprotective nanostructured formulations for UV protection and antioxidant activity. Ind Crop Prod. 2015;67:18–24.

11. Hora JJ, Maydew ER, Lansky EP, Dwivedi C. Chemopreventive effects of pomegranate seed oil on skin tumor development in CD1 mice. J Med Food. 2004;12:151–6.

12. Ferreira LM, Cervi VF, Gehrcke M, da Silveira EF, Azambuja JH, Braganhol E, et al. Ketoprofen-loaded pomegranate seed oil nanoemulsion stabilized by pullulan: selective antiglioma formulation for intravenous administration. Colloids Surf B Biointerfaces. 2015;130:272–7.

13. Ferreira LM, Gehrcke M, Cervi VF, Bitencourt PER, da Silveira EF, Azambuja JH, et al. Pomegranate seed oil nanoemulsions with selective antiglioma activity: optimization and evaluation of cytotoxicity, genotoxicity and oxidative effects on mononuclear cells. Pharm Biol. 2016;209–20.

14. Mizrahi M, Friedman-Levi Y, Larush L, Frid K, Binyamin O, Dori D, et al. Pomegranate seed oil nanoemulsions for the prevention and treatment of neurodegenerative diseases: the case of genetic CJD. Nanomed Nanotechnol Biol Med. 2014;10:1353–63.

15. Niculae G, Lacatusu I, Badea N, Meghea A, Stan R. Influence of vegetable oil on the synthesis of bioactive nanocarriers with broad spectrum photoprotection. Cent Eur J Chem. 2014;12:837–50.

16. Lu LY, Liu Y, Zhang ZF, Gou XJ, Jiang JH, Zhang JZ, et al. Pomegranate seed oil exerts synergistic effects with trans-resveratrol in a self-nanoemulsifying drug delivery system. Biol Pharm Bull. 2015;38:1658–62.

17. Ferreira LM, Sari MHM, Cervi VF, Gehrcke M, Barbieri AV, Zborowski VA, et al. Pomegranate seed oil nanoemulsions improve the photostability and in vivo antinociceptive effect of a non-steroidal anti-inflammatory drug. Colloids Surf B Biointerfaces. 2016;144:214–21.

18. Frank LA, Contri RV, Beck RCR, Pohlmann AR, Guterres SS. Improving drug biological effects by encapsulation into polymeric nanocapsules. WIREs Nanomed Nanobiotechnol. 2015;7:623–39.

19. Chassot JM, Ribas D, Silveira EF, Grünspan LD, Pires CC, Farago PV, et al. Beclomethasone dipropionate-loaded polymeric nanocapsules: development, in vitro cytotoxicity and in vivo evaluation of acute lung injury. J Nanosci Nanotechnol. 2015;15:855–64.

20. Santos SS, Lorenzoni A, Pegoraro NS, Denardi LB, Alves SH, Schaffazick SR, et al. Formulation and in vitro evaluation of coconut oil-core cationic nanocapsules intended for vaginal delivery of clotrimazole. Colloids Surf B Biointerfaces. 2014;116:270–6.

21. Contri RV, Kulkamp-Guerreiro IC, da Silva SJ, Frank LA, Pohlmann AR, Guterres SS. Nanoencapsulation of rose-hip oil prevents oil oxidation and allows obtainment of gel and film topical formulations. AAPS PharmSciTech. 2015;17:863–71.

22. Maluf SW, Riegel M. Citogenética humana. 1rd ed. Porto Alegre: Artmed; 2011.

23. Marchiori MCLM, Rigon C, Camponogara C, Oliveira SM, Cruz L. Hydrogel containing silibinin-loaded pomegranate oil based nanocapsules exhibits anti-inflammatory effects on skin

24. Guterres SS, Weiss V, Freitas LDL, Pohlmann AR. Influence of benzyl benzoate as oil core on the physicochemical properties of spray-dried powders from polymeric nanocapsules containing indomethacin. Drug Deliv. 2000;7:195–9.

25. Fessi H, Puisieux F, Devissaguet JP, Ammoury N, Benita S. Nanocapsule formation by interfacial polymer deposition following solvent displacement. Int J Pharm. 1989;55:1–4.

26. Korsmeyer RW, Gurny R, Doelker E, Buri P, Peppas NA. Mechanisms of solute release from porous hydrophilic polymers. Int J Pharm. 1983;15:25–35.

27. Serpen A, Capuano E, Fogliano V, Gökmen V. A new procedure to measure the antioxidant activity of insoluble food components. J Agric Food Chem. 2007;55:7676–81.

28. Garcia O, Mandina T, Lamadrid AI, Diaz A, Remigio A, Gonzalez Y, et al. Sensitivity and variability of visual scoring in the comet assay. Results of an inter-laboratory scoring exercise with the use of silver staining. Mutat Res. 2004;556:25–34.

29. Quinteros D, Ferreira LM, Schaffazick SR, Palma SD, Allemandi DA, Cruz L. Novel polymeric nanoparticles intended for ophthalmic administration of acetazolamide. J Pharm Sci. 2016;10:3183–90.

30. Marchiori ML, Lubini G, Dalla Nora G, Friedrich RB, Fontana MC, Ourique AF, et al. Hydrogel containing dexamethasone-loaded nanocapsules for cutaneous administration: preparation, characterization, and in vitro drug release study. Drug Dev Ind Pharm. 2010;36:962–71.

31. Sahu S, Saraf S, Kaur CD, Saraf S. Biocompatible nanoparticles for sustained topical delivery of anticancer phytoconstituent quercetin. Pak J Biol Sci. 2013;16:601–9.

32. Hung C, Lin Y, Zhang L, Chang C, Fang J. Topical delivery of silymarin constituents via the skin route. Acta Pharmacol Sin. 2010;31:118–26.

33. Korkina LG, Pastore S, De Luca C, Kostyuk VA. Metabolism of plant polyphenols in the skin: beneficial versus deleterious effects. Curr Drug Metab. 2008;9:710–29.

34. Lokhande AB, Mishra S, Kulkarni RD, Naik JB. Preparation and characterization of repaglinide loaded ethylcellulose nanoparticles by solvent diffusion technique using high pressure homogenizer. J Pharm Res. 2013;7:421–6.

35. Pyszková M, Biler M, Biedermann D, Valentová K, Kuzma M, Vrba J, et al. Flavonolignan 2,3-dehydroderivatives: preparation, antiradical and cytoprotective activity. Free Radic Biol Med. 2016;90:114–25.

36. Ourique AF, Chaves PDS, Souto GD, Pohlmann AR, Guterres SS, Beck RCR. Redispersible liposomal-N-acetylcysteine powder for pulmonary administration: development, in vitro characterization and antioxidant activity. Eur J Pharm Sci. 2014;65:174–82.

37. Gehrcke M, Giuliani LM, Ferreira LM, Barbieri AV, Sari MHM, Silveira EF, et al. Enhanced photostability, radical scavenging and antitumor activity of indole-3-carbinol-loaded rose hip oil nanocapsules. Mater Sci Eng. 2016; doi:10.1016/j.msec.2016.12.006.

38. Jahan N, Aslam S, Rahman KU, Fazal T, Anwar F, Saher R. Formulation and characterisation of nanosuspension of herbal extracts for enhanced antiradical potential. J Exp Nanosci. 2015;11:72–80.

39. Calligaris S, Comuzzo P, Bot F, Lippe G, Zironi R, Anese M, et al. Nanoemulsions as delivery systems of hydrophobic silybin from silymarin extract: effect of oil type on silybin solubility, in vitro bioaccessibility and stability. LWT - Food Sci Technol. 2015;63:77–84.

40. Bannwart CF, Peracoli JC, Takahagi EN, Peracoli MT. Inhibitory effect of silibinin on tumour necrosis factor-alpha and hydrogen peroxide production by human monocytes. Nat Prod Res. 2010;24:1747–57.

41. Bannwart CF, Takahagi EN, Golim MA, de Medeiros LTL, Romão M, Weel IC, et al. Downregulation of nuclear factor-kappa B (NF-κB) pathway by silibinin in human monocytes challenged with Paracoccidioides brasiliensis. Life Sci. 2010;86:880–6.

42. Cristofalo R, Bannwart-Castro CF, Magalhães CG, Borges VTM, Peraçoli JC, Witkin SS, et al. Silibinin attenuates

damage UVB radiation-induced in mice. J Photochem Photobiol B. 2017;170:25–32.

oxidative metabolism and cytokine production by monocytes from preeclamptic women. Free Radic Res. 2013;47:268–75.

43. Dalle-Donne I, Rossi R, Giustarini D, Milzani A, Colombo R. Protein carbonyl groups as biomarkers of oxidative stress. Clin Chim Acta. 2003;329:23–38.

44. Sati J, Mohanty BP, Garg ML, Koul A. Pro-oxidant role of silibinin in DMBA/TPA induced skin cancer: ^{1}H NMR metabolomic and biochemical study. PLoS One. 2016; doi:10.1371/journal.pone.0158955.

45. Bonez PC, Ramos AP, Nascimento K, Copetti PM, Souza ME, Rossi GG, *et al*. Antibacterial, cyto and genotoxic activities of A22 compound ((S-3, 4 -dichlorobenzyl) isothiourea hydrochloride). Microb Pathog. 2016;99:14–8.

46. Ahlenstiel T, Burkhardt G, Köhler H, Kuhlmann MK. Bioflavonoids attenuate renal proximal tubular cell injury during cold preservation in Euro-Collins and University of Wisconsin solutions. Kidney Int. 2003;63:554–63.